GEOLOGY | THE GEOLOGICAL SOCIETY OF AMERICA®

https://doi.org/10.1130/G48388.1

Manuscript received 13 September 2020
Revised manuscript received 18 December 2020
Manuscript accepted 24 December 2020

Published online 4 March 2021

Volcanic carbon cycling in East Lake, Newberry Volcano, Oregon, USA

H.D. Brumberg[1,2], L. Capece[1], C.N. Cauley[1], P. Tartell[1], C. Smith[1], M.S. Wagner[1] and J.C. Varekamp[1]
[1]Department of Earth and Environmental Sciences, Wesleyan University, Middletown, Connecticut 06459, USA
[2]Osa Conservation, Washington, D.C. 20005, USA

ABSTRACT

The carbon cycle in East Lake (Newberry Volcano, Oregon, USA) is fueled by volcanic CO_2 inputs with traces of Hg and H_2S. The CO_2 dissolves in deep lake waters and is removed in shallow waters through largely diffusive surface degassing and photosynthesis. Escaping gas and photosynthate have low $\delta^{13}C$ values, leading to $\delta^{13}C$(DIC) (DIC—dissolved inorganic carbon) as high as +5.7‰ in surface waters, well above the common global lake range. A steep $\delta^{13}C$ depth gradient is further established by respiration and absorption of light volcanic CO_2 in bottom waters. The seasonal CO_2 degassing starts at >100 t CO_2/day after ice melting in the spring and declines to ~40 t/day in late summer, degassing ~11,700 t CO_2/yr. Thus, volcano monitoring through gas fluxes from crater lakes should consider lacustrine processes that modulate the volcanic gas output over time. The flux contribution of a bubbling CO_2 "hotspot" increased from 20% to >90% of the lake-wide CO_2 flux from 2015 to 2019 CE, followed by a "toxic gas alert" in July 2020. East Lake is an active volcanic lake with a "geogenic" ecosystem driven primarily by hydrothermal inputs.

INTRODUCTION

Some volcanic lakes have active CO_2 inputs (e.g., Chiodini et al., 2012; Christenson and Tassi, 2015), and a few have experienced explosive episodes in the past (e.g., Lake Nyos, Cameroon; Kusakabe, 2017). Volcanic CO_2 negatively impacts some oceanic ecosystems (e.g., Carey et al., 2013; Price et al., 2015), and CO_2 emissions in the volcanic Mammoth Lakes (California, USA) area (e.g., Bergfeld et al., 2006) kill local forests. However, some ecosystems utilize volcanic inputs (Cabassi et al., 2013). The incoming volcanic CO_2 is processed by the lentic ecosystem, but most of it escapes through surface degassing (e.g., Caudron et al., 2012; Andrade et al., 2016). This CO_2 lake flux is commonly used in volcano monitoring (e.g., Rouwet et al., 2014; Mazot and Bernard, 2015; Varekamp, 2015).

Newberry Volcano (Oregon, USA; 43.728°N, 121.210°W) is a Cascade Range back-arc volcano (Carlson et al., 2018), most recently active 1300 yr ago, with two small crater lakes aged ca. 7.5 ka (Jensen and Donnelly-Nolan, 2017). East Lake is a drowned crater with visual evidence of CO_2 inputs from the lake bottom (Lefkowitz et al., 2017). The CO_2 bubbles carry traces of H_2S and Hg gas but almost no fluids. A bubbly CO_2-Hg-H_2S "hotspot" is found along the southeastern beach (Fig. 1). East Lake has no inlets or outlets, a maximum water depth of 55 m, and a 4.2 km^2 surface area. It is frozen in winter and thermally stratified in summer (Lefkowitz et al., 2017). This study aims to determine the magnitude of the volcanic CO_2 input in this carbonate-rich volcanic lake based on 5 years of flux measurements and to map the local carbon cycle based on carbon isotope evidence.

METHODS

We measured lake surface CO_2 fluxes using an accumulation float chamber (e.g., Mazot and Bernard, 2015) and a LI-COR CO_2 detector (model LI-6252). Field samples and measurements were collected annually between June and August from 2015 to 2019, with additional data collected in May 2018 shortly after ice melting. The field data points were treated with sequential Gaussian simulations (SGSs; Cardellini et al., 2003) to estimate lake-wide CO_2 release rates. Gas samples from the accumulation chamber and ambient CO_2 from air on land and from above the lake were injected into pre-evacuated Exetainer vials for stable isotope analyses. Gas bubbles in the hot-spring pools were collected through water displacement in inverted plastic bottles. Lake depth profiles for pH and temperature were obtained with a YSI Professional Plus five-probe analyzer. Lake water samples were taken at 10 m depth intervals with a Teflon Wildco 2 L water sampler and stored in Exetainers for $\delta^{13}C$(DIC) (DIC—dissolved inorganic carbon) analyses after filtration (0.2 μm). Additional details on methods are provided in the Supplemental Material[1].

RESULTS

The CO_2 escape rates measured between late June and August were similar in 2015–2019, with average CO_2 fluxes of ~0.2 mol/m^2/day. The SGS data treatment provided a mean value of 46 ± 10 t CO_2/day as the typical summer CO_2 evasion rate (Fig. S1 and Table S1 in the Supplemental Material). The bubbly CO_2 "hotspot" increased in size and intensity over 2015–2019 without impacting the overall flux (see the Supplemental Material). The hotspot flux contribution increased from 20% to >90% of the lake-wide CO_2 flux, which culminated in a "gas alert'" in July 2020 (USGS, 2020). The mid-May 2018 CO_2 flux was ~95 t CO_2/day, well outside the summer range and with a different spatial flux pattern. More than 50% of the lake area was emitting >0.5 mol/m^2/day, whereas the other surveys reached such values over ~15% of the lake area only, largely in the hotspot area.

[1]Supplemental Material. Details on the laboratory, data analysis, modeling methods, and equipment specifications, including methods and results of the two box models showing seasonal carbon cycling in East Lake, and raw data from the main text figures. Please visit https://doi.org/10.1130/GEOL.S.14046902 to access the supplemental material, and contact editing@geosociety.org with any questions.

CITATION: Brumberg, H.D., et al., 2021, Volcanic carbon cycling in East Lake, Newberry Volcano, Oregon, USA: Geology, v. 49, p. 718–722, https://doi.org/10.1130/G48388.1

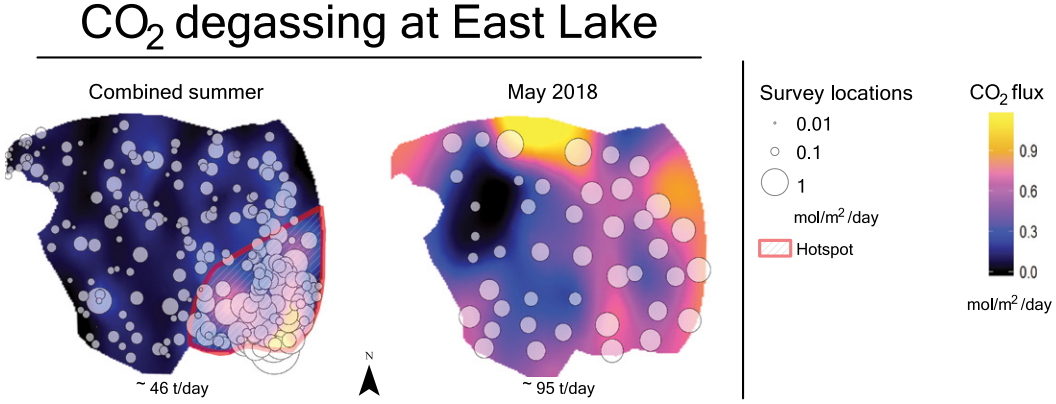

Figure 1. Five-year time-integrated summer CO_2 flux pattern at East Lake (Oregon, USA; 43.7306°N, 121.2098°W), combining 256 flux measurements, compared to the pattern in May 2018. Sample point sizes are scaled to measured flux. Sequential Gaussian simulation color scale is located to the right. Hotspot region is outlined in red. In May 2018, the flux had a different distribution pattern and larger overall flux. There were many zones of high CO_2 flux, and the hotspot no longer stood out.

Gas samples, with 420–800 ppm CO_2, taken from the float chamber during CO_2 accumulation runs, are mixtures of ambient and lake CO_2, with $\delta^{13}C(CO_2)$ from −8‰ to −17‰ (Fig. 2). The $\delta^{13}C(CO_2)$ in ambient gas samples (air) ranged from the fully mixed atmospheric value of ~−8.7 ‰ at ~410 ppm CO_2 (NOAA, 2020) to values of −17‰ at 700 ppm CO_2. In some experiments, we pumped the air component out of the chamber and after some accumulation time, the chamber contained only lake gas, with $\delta^{13}C(CO_2)$ values of −9‰ to −15‰. The $\delta^{13}C(CO_2)$ of hot-spring bubbles ranged from −3‰ to −8‰ (Table S2).

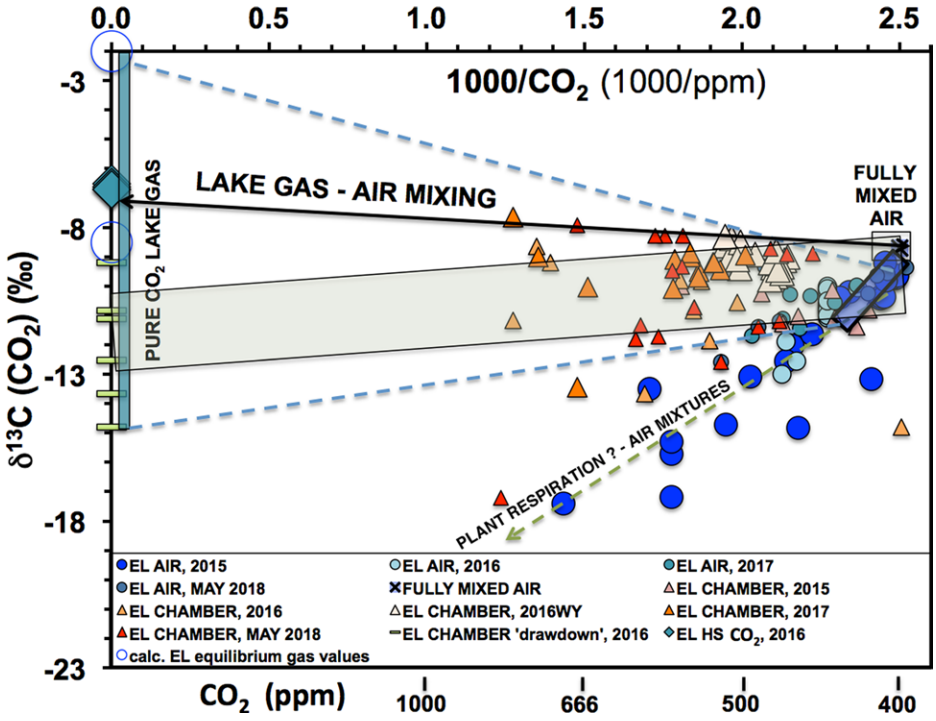

Figure 2. Keeling mixing diagram with concentrations and $\delta^{13}C$ values of CO_2 in ambient air (filled circles) and in accumulation chamber gas (triangles) from our sampling campaign at East Lake (EL; Oregon, USA; 43.7306°N, 121.2098°W). $\delta^{13}C$ values of "pure lake gas" plot at zero on the x-axis. Air plots on the right-hand side of diagram (~400 ppm), with blue bar indicating the range of $\delta^{13}C$ values from air samples taken 5–15 km upwind from the lake. Air data array represents mixing between common air and plant respiration, boat exhaust gas, lake gas above the lake surface, and possibly forest-fire CO_2. Large blue open circles represent predicted equilibrium isotope compositions of lake gas. Light-green "drawdown" symbols (flat bars) stem from experiments where ambient CO_2 had been pumped out of the chamber. Chamber data represent mixtures of ambient CO_2 and possible lake gas compositions (vertical teal bar). The 2016WY data were analyzed at the University of Wyoming (USA), all other data are from the University of California–Davis (USA); HS samples refer to CO_2 bubbles collected from hot springs. Likely mixing array that covers ~75% of the data is shown with a pale green band, indicating mixing of slightly contaminated air with "pure lake gas" that has $\delta^{13}C$ values of –10‰ to –12.5‰. Thick black line represents mixing between standard fully mixed atmospheric CO_2 with an equilibrium lake gas (HS sample); dashed light-blue mixing lines represent the possible extremes of air-lake gas mixing; dashed green line is the air CO_2–biogenic CO_2 mixing line.

Surface-water pH values varied over the years of record from ~7.4 in May to 8 in September, with pH values down to ~6.4 in the hypolimnion. Lake-water profiles show increasing DIC and conductivity with depth (Lefkowitz et al., 2017), mainly due to CO_2 gain from volcanic CO_2 absorption and respiration at depth and CO_2 loss from diffusive CO_2 escape and photosynthesis in the epilimnion.

The $\delta^{13}C(DIC)$ in the epilimnion varied over the years of the survey from +2.5‰ to +5.7‰, with May 2018 at 3.5‰ and the highest values in late summer (Table S3). Hypolimnial values were lower and ranged from −0.5‰ to +4‰ (Fig. 3). The isotopic depth gradient [$\Delta\delta^{13}C(DIC)$] also differed over the season, with the smallest $\Delta\delta^{13}C(DIC)$ values in May 2018 and June 2015–2016 (0.5‰–1‰), and the largest (4‰–5‰) in late summer over the years surveyed (Fig. 3).

The ^{14}C contents of DIC in surface water and at 42 m depth collected in summer 2015 (Table S4) was 24.7% and 28.8% of modern ^{14}C, respectively, both much lower values than in lakes in open exchange with the atmosphere (e.g., Taibei et al., 2018).

East Lake sediment carries 2%–12% C_{org} (org—organic) from diatoms, cyanobacteria, and subaquatic vegetation debris (SAV). Cores taken near the CO_2-rich bubbling zone have the highest C_{org} (8%–12%; see the Supplemental Material). The $\delta^{13}C(C_{org})$ ranges from −17‰ (rich in SAV) to −24‰, with a mean value of −23‰ in surface sediments (Lefkowitz et al., 2017). Mercury concentrations in cores and grab samples throughout the lake range from 0.5 to 4 ppm Hg (Lefkowitz et al., 2017), whereas cores in and around the hotspot have 3–13 ppm Hg (see the Supplemental Material).

DISCUSSION

The data provide a 5 yr record of carbon cycling in East Lake, with implications for its ecosystem functioning and volcano monitoring. Spring melting of the winter ice cover leads to lake overturn, intense CO_2 degassing

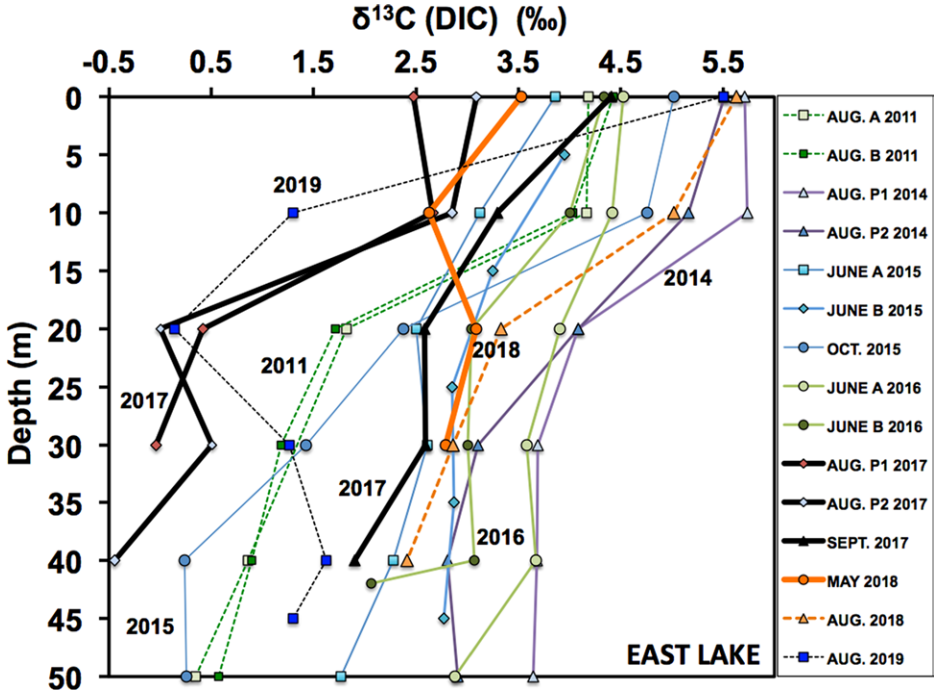

Figure 3. Depth versus δ¹³C(DIC) (DIC—dissolved inorganic carbon) trends at East Lake Oregon, USA (43.7306°N, 121.2098°W) over several years, taken in different months (May–August). A, B, P1, and P2 refer to different locations of depth profiles taken in the same sampling year. Slopes are variable: almost vertical in May, and stronger gradients in August. Thick black and orange lines are discussed in the text.

(>100 t CO_2/day), and the onset of algal productivity. In the fall, the CO_2 flux diminishes to <40 t/day, then the lake again turns over, followed by freezing of surface waters with the cessation of photosynthesis and CO_2 surface degassing. During the winter, the lake accumulates dissolved volcanic CO_2.

We fitted a power-law function to the CO_2 flux data (Fig. 4) to model seasonal CO_2 escape rates (Supplemental Material), showing that excess winter CO_2 is "blown off" from April through late August. In late summer, the lake evolves toward a steady state with volcanic CO_2 output roughly equaling the volcanic input, estimated at ~32 t CO_2/day year-round (Supplemental Material). The lake CO_2 loss of ~11,700 t/yr is comparable to those from other similarly sized volcanic lakes (Pérez et al., 2011). Over these 5 yr of study, the hotspot growth was most likely caused by a drop in lake level, driven by higher ambient temperatures and lower precipitation levels (NIDIS, 2020). A lower lake level created a larger area across which bubbles could reach the surface and discharge directly into the atmosphere. The 2020 "gas alert" thus was not driven by deep-seated volcanic degassing processes (USGS, 2020).

East Lake has high epilimnial δ¹³C(DIC) values compared to typical global δ¹³C(DIC) lake values (−20‰ to 0‰; Bade et al., 2004) but similar to some other CO_2-degassing carbonate-rich volcanic lakes (e.g., Mazot et al., 2014). High δ¹³C(DIC) occurs in nonvolcanic lakes with extensive methane generation (e.g., Gu et al., 2004) or strong seasonal algal blooms (e.g., Oren et al., 1995), which are both absent in East Lake. Δδ¹³C(DIC) broadly increases over the season as a result of increasing δ¹³C(DIC) in surface waters and decreasing δ¹³C(DIC) in deeper waters. δ¹³C(DIC) in the epilimnion can increase by ~2‰ (e.g., between May and August 2018), while deep-water δ¹³C(DIC) can decrease by several per mil after spring homogenization. Δδ¹³C(DIC) is created by photosynthesis and CO_2 degassing in the epilimnion and by respiration and addition of low-δ¹³C volcanic CO_2 in the hypolimnion. The δ¹³C(DIC) depth profiles show the fully developed gradient in August 2017, a lesser gradient in September (storm-related lake mixing), and then near fully mixed conditions in May 2018 after ice melting, indicative of lake turnover (Fig. 3, thick black and orange lines).

The ¹⁴C(DIC) data provide apparent water ages of >10,000 yr (Table S4), but East Lake is only 6500 yr old. Water-budget modeling suggests a water residence time of ~20 yr (Lefkowitz et al., 2017). The CO_2-degassing surface waters do not equilibrate with atmospheric CO_2, and the large flux of "dead" volcanic CO_2 strongly dilutes the atmospheric ¹⁴C input that presumably enters the lake largely through precipitation.

The measured δ¹³C(CO_2) values from the accumulation chamber range from −8‰ to −17‰ and cannot be explained as binary mixtures of lake CO_2 gas in equilibrium with lake DIC and fully mixed atmospheric ambient CO_2 (−8.7‰). Equilibrium δ¹³C(CO_2) values for lake gas were calculated from isotope mass-balance statements, temperature-dependent intra-species fractionation factors (DeVries et al., 2001), and speciation calculations using the program CO_2Sys (Pierrot and Wallace, 2006). The epilimnial δ¹³C(DIC) values (+2.5‰ to +5.7‰), temperature (0–18 °C), and pH (7–8.2) provided δ¹³C(CO_2) equilibrium values of −2.5‰ to −8.5‰.

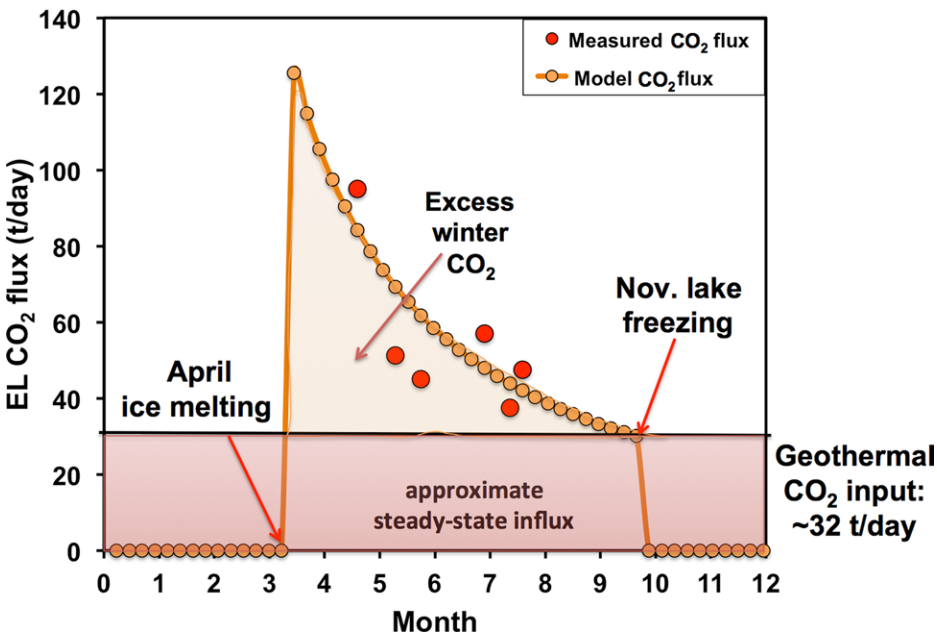

Figure 4. Seasonal CO_2 degassing trend at East Lake (EL; Oregon, USA; 43.7306°N, 121.2098°W) with best fit power-law trend to lake-wide average flux.

Binary mixing of standard ambient air with an equilibrium lake gas composition of −7‰ $\delta^{13}C(CO_2)$ would create a mixing line at the upper section of the data array (Fig. 2, thick black line). Our analyses of local ambient air show a range between fully standard air and a low-$\delta^{13}C$ component, such as forest and/or ground respiration CO_2 at ~-27‰ (Bowling et al., 2002; Chiodini et al., 2008, 2011). Newberry summer nights can be below freezing, leading to the formation of a nocturnal atmospheric boundary layer. Soil and forest CO_2 emissions trapped in the atmospheric ground layer may create the observed low $\delta^{13}C$ values in CO_2-enriched air (Fig. 2). In addition, low-$\delta^{13}C$ CO_2 may have been contributed by the common regional forest fires and powerboat exhaust gases, and air collected above the lake may have a lake gas component. The range in $\delta^{13}C(CO_2)$ of potential pure lake gas samples (Fig. 2, teal green bar) spans the calculated equilibrium gas values and the "pure lake gas" chamber samples (light green bar symbols). The latter may be explained with a kinetic isotope effect relative to the calculated equilibrium values. Mixing between the "pure lake gas" samples and slightly contaminated air covers the majority of data points (pale green band), but this solution is not unique.

Thus, the escaping CO_2 has low $\delta^{13}C$ values, with $\delta^{13}C(CO_2)$ a function of lake composition and a degree of kinetic fractionation that usually depends on the wind speed. The loss of this CO_2 gas is one driver for the heavy $\delta^{13}C$(DIC) in shallow waters and the depth gradients that build up over the season.

The second carbon sink from the epilimnion is the photosynthetic flux, which we constrain by the C_{org} burial rate. Only a fraction of the photosynthetic flux is buried; the rest is recycled in the hypolimnion through respiration and oxidation (Cole et al., 1994). Primary organic productivity thus also depletes the DIC in ^{12}C in epilimnial waters. We calculated the C_{org} burial rate from C_{org} data, the mean sediment mass accretion rate (~0.05 g/cm^2/yr) based on core-top ^{210}Pb ages (Lefkowitz et al., 2017) and a volcanic ash age deeper in one core (ca. 1300 yr B.P. Paulina Lake ash flow layer; Jensen and Donnelly-Nolan, 2017), and bulk dry sediment density data. The mean lake C_{org} burial rate is ~3.3 mg C/cm^2/yr, translating into a lake-wide C_{org} burial rate of 140 ± 30 t C/yr.

A preliminary two-box model using the measured carbon fluxes and calculated equilibrium isotope fractionation factors shows that the calculated $\delta^{13}C$(DIC) values and isotope gradients broadly match the whole observed $\delta^{13}C$(DIC) spectrum (Supplemental Material). The data and modeling indicate that diffusive CO_2 degassing strongly contributes to $\Delta\delta^{13}C$(DIC). A carbon-isotope depth gradient is thus not a precise indicator of primary lake productivity (e.g., McKenzie, 1985) if surface CO_2 degassing occurs as well.

The CO_2-rich hot-spring bubbles possibly contain primary volcanic CO_2 as suggested by He mantle isotope values (ratio relative to the atmospheric value, R_a, = 7.6–8.3; Graham et al., 2009). The $\delta^{13}C(CO_2)$ in discrete bubbles was determined at −3‰ to −8‰, and the box modeling (see the Supplemental Material) demands an input value of ~-6‰ to −7‰, close to general mantle CO_2 values (Deines and Gold, 1973).

The phosphorus for photosynthesis and silicon for diatom frustule construction are supplied by the geothermal fluids, and fixed nitrogen is supplied by diazotroph cyanobacteria (Lefkowitz et al., 2017). The high levels of CO_2 may stimulate the local primary productivity (Hamdan et al., 2018), and the CO_2-rich hotspot area has the highest C_{org} contents (as much as 12%; see the Supplemental Material).

Consequently, the lake ecosystem benefits from hydrothermal inputs and is highly productive (6%–12% C_{org} in ash-poor sediment). The high sedimentary Hg levels (Lefkowitz et al., 2017) have no major deleterious impact on the ecosystem, although plankton tows yielded 5 ppm Hg and fish with low parts-per-million Hg values (see the Supplemental Material).

CONCLUSIONS

East Lake is not a North American version of Lake Nyos in Cameroon, where CO_2 accumulated over decades until a catastrophic release took place (e.g., Kusakabe, 2017). At East Lake, accumulated winter CO_2 is released every year during spring and summer. Seasonal ice cover blocking diffusional CO_2 escape occurs in many high-latitude and high-altitude lakes (e.g., Cole et al., 1994). This delay in the release of winter CO_2 may mute the seasonal oscillation in atmospheric CO_2 (Tranvik et al., 2009). Volcano monitoring through gas flux measurements in volcanic lakes must account for lacustrine processes that modulate the gas flux, especially when ice cover occurs. During low-wind periods, the lake is most likely degassing CO_2 with low $\delta^{13}C(CO_2)$ as a result of kinetic fractionation during degassing, whereas during windy periods, the CO_2 flux increases (see the Supplemental Material) and $\delta^{13}C(CO_2)$ becomes close to the equilibrium isotopic composition. The accumulation-chamber data are not an exact replica of natural CO_2 degassing because of the protected environment inside the chamber.

East Lake has a "geogenic" ecosystem that is almost entirely fed by volcanic nutrients, including CO_2. Its waters have high $\delta^{13}C$(DIC) values due to CO_2 degassing and photosynthesis. East Lake's system is dualistic in nature with a hydrothermal supply of good nutrients and harmful toxins, where the good far outpaces the bad for the ecosystem.

ACKNOWLEDGMENTS

Field support was provided by Ellen Thomas, Sabrina Koetter, Haley Brumberger, Jim Zareski, Scott Herman, and the staff of East Lake Resort (La Pine, Oregon, USA). Daniele McKay (University of Oregon, Eugene, Oregon) and her students took samples in the late fall. Peter Raymond (Yale University, New Haven, Connecticut) provided the ^{14}C analyses. Communications with the Volcanic Hazards branch of the U.S. Geological Survey (USGS) on the 2020 Newberry volcano gas alert were informative and highly appreciated. Particular thanks to Jen Lewicki (USGS) for running an informal sequential Gaussian simulation on the 2019 data. Funding was provided by Wesleyan University, Connecticut (Stearns Chair Fund to Varekamp); Keck Consortium, Minnesota (2015, grant NSF-REU 1358987); Connecticut Space Grant Consortium/NASA (awards P-1268-2017 to Wagner and P-1323-2018 to Cauley); and a Mazamas (Oregon) Outdoor Education Foundation grant (2017, to Wagner). We thank three anonymous reviewers for their insightful comments on the manuscript.

REFERENCES CITED

Andrade, C., Viveiros, F., Cruz, J.V., Coutinho, R., and Silva, C., 2016, Estimation of the CO_2 flux from Furnas volcanic lake (São Miguel, Azores): Journal of Volcanology and Geothermal Research, v. 315, p. 51–64, https://doi.org/10.1016/j.jvolgeores.2016.02.005.

Bade, D.L., Carpenter, S.R., Cole, J.J., Hanson, P.C., and Hesslein, R.H., 2004, Controls of $\delta^{13}C$-DIC in lakes: Geochemistry, lake metabolism, and morphometry: Limnology and Oceanography, v. 49, p. 1160–1172, https://doi.org/10.4319/lo.2004.49.4.1160.

Bergfeld, D., Evans, W.C., Howle, J.F., and Farrar, C.D., 2006, Carbon dioxide emissions from vegetation-kill zones around the resurgent dome of Long Valley caldera, eastern California, USA: Journal of Volcanology and Geothermal Research, v. 152, p. 140–156, https://doi.org/10.1016/j.jvolgeores.2005.11.003.

Bowling, D.R., McDowell, N.G., Bond, B.J., Law, B.E., and Ehleringer, J.R., 2002, ^{13}C content of ecosystem respiration is linked to precipitation and vapor pressure deficit: Oecologia, v. 131, p. 113–124, https://doi.org/10.1007/s00442-001-0851-y.

Cabassi, J., Tassi, F., Vaselli, O., Fiebig, J., Nocentini, M., Capecchiacci, F., Rouwet, D., and Bicocchi, G., 2013, Biogeochemical processes involving dissolved CO_2 and CH_4 at Albano, Averno, and Monticchio meromictic volcanic lakes (Central–Southern Italy): Bulletin of Volcanology, v. 75, 683, https://doi.org/10.1007/s00445-012-0683-0.

Cardellini, C., Chiodini, G., and Frondini, F., 2003, Application of stochastic simulation to CO_2 flux from soil: Mapping and quantification of gas release: Journal of Geophysical Research, v. 108, 2425, https://doi.org/10.1029/2002JB002165.

Carey, S., Nomikou, P., Bell, K.C., Lilley, M., Lupton, J., Roman, C., Stathopoulo, B., Beielou, K., and Ballard, R., 2013, CO_2 degassing from hydrothermal vents at Kolumbo submarine volcano, Greece, and the accumulation of acidic crater water: Geology, v. 41, p. 1035–1038, https://doi.org/10.1130/G34286.1.

Carlson, R.W., Grove, T.L., and Donnelly-Nolan, J.M., 2018, Origin of primitive tholeiitic and calc-alkaline basalts at Newberry Volcano, Oregon: Geochemistry Geophysics Geosystems, v. 19, p. 1360–1377, https://doi.org/10.1029/2018GC007454.

Caudron, C., Mazot, A., and Bernard, A., 2012, Carbon dioxide dynamics in Kelud volcanic lake:

Journal of Geophysical Research, v. 117, B05102, https://doi.org/10.1029/2011JB008806.
Chiodini, G., Caliro, S., Cardellini, C., Avino, R., Granieria, D., and Schmidt, A., 2008, Carbon isotopic composition of soil CO_2 efflux: A powerful method to discriminate different sources feeding soil CO_2 degassing in volcanic-hydrothermal areas: Earth and Planetary Science Letters, v. 274, p. 372–379, https://doi.org/10.1016/j.epsl.2008.07.051.
Chiodini, G., Caliro, S., Aiuppa, A., Avino, R., Granieri, D., Moretti, R., and Parello, F., 2011, First $^{13}C/^{12}C$ isotopic characterisation of volcanic plume CO_2: Bulletin of Volcanology, v. 73, p. 531–542, https://doi.org/10.1007/s00445-010-0423-2.
Chiodini, G., Tassi, F., Caliro, S., Chiarabba, C., Vaselli, O., and Rouwet, D., 2012, Time-dependent CO_2 variations in Lake Albano associated with seismic activity: Bulletin of Volcanology, v. 74, p. 861–871, https://doi.org/10.1007/s00445-011-0573-x.
Christenson, B., and Tassi, F., 2015, Gases in volcanic lake environments, *in* Rouwet, D., et al., eds. Volcanic Lakes: Berlin, Heidelberg, Springer Media Publishers, p. 737–753
Cole, J.J., Caraco, N.F., Kling, G.W., and Kratz, T.K., 1994, Carbon dioxide supersaturation in the surface waters of lakes: Science, v. 265, p. 1568–1570, https://doi.org/10.1126/science.265.5178.1568.
Deines, P., and Gold, D.P., 1973, Isotopic composition of carbonatite and kimberlite carbonates and their bearing on isotopic composition of deep-seated carbon: Geochimica et Cosmochimica Acta, v. 37, p. 1709–1733, https://doi.org/10.1016/0016-7037(73)90158-0.
DeVries, J.J., 2001, Environmental Isotopes in the Hydrological Cycle: Volume 1: Principles and Applications: International Atomic Energy Agency and United Nations Educational, Scientific and Cultural Organization (IAEA-UNESCO): http://www-naweb.iaea.org/napc/ih/documents/global_cycle/Environmental%20Isotopes%20in%20the%20Hydrological%20Cycle%20Vol%201.pdf.
Graham, D.W., Reid, M.R., Jordan, B.T., Grunder, A.L., Leeman, W.P., and Lupton, J.E., 2009, Mantle source provinces beneath the Northwestern USA delimited by helium isotopes in young basalts: Journal of Volcanology and Geothermal Research, v. 188, p. 128–140, https://doi.org/10.1016/j.jvolgeores.2008.12.004.
Gu, B., Schelske, C.L., and Hodell, D.A., 2004, Extreme ^{13}C enrichments in a shallow hypereutrophic lake: Implications for carbon cycling: Limnology and Oceanography, v. 49, p. 1152–1159, https://doi.org/10.4319/lo.2004.49.4.1152.
Hamdan, M., Byström, P., Hotchkiss, E.R., Al-Haidarey, M., Ask, J., and Karlsson, J., 2018, Carbon dioxide stimulates lake primary production: Scientific Reports, v. 8, 10878, https://doi.org/10.1038/s41598-018-29166-3.
Jensen, R.A., and Donnelly-Nolan, J.M., 2017, Field-trip guide to the geologic highlights of Newberry Volcano, Oregon: U.S. Geological Survey Scientific Investigations Report 2017-5022-J2, 30 p., https://doi.org/10.3133/sir20175022J2.
Kusakabe, M., 2017, Lakes Nyos and Monoun Gas Disasters (Cameroon)—Limnic Eruptions Caused by Excessive Accumulation of Magmatic CO_2 in Crater Lakes: Tokyo, TERRAPUB, Geochemistry Monograph Series, v. 1, 50 p., https://doi.org/10.5047/gems.2017.00101.0001.
Lefkowitz, J.N, Varekamp, J.C., Reynolds, R.W., and Thomas, E., 2017, A tale of two lakes: The Newberry Volcano twin crater lakes, Oregon, USA, *in* Ohba, T., et al., eds., Geochemistry and Geophysics of Active Volcanic Lakes: Geological Society of London Special Publication 437, p. 253–288, https://doi.org/10.1144/SP437.15.
Mazot, A., and Bernard, A., 2015, CO_2 degassing from volcanic lakes, *in* Rouwet, D., et al., eds. Volcanic Lakes: Berlin, Heidelberg, Springer Media Publishers, p. 341– 354, https://doi.org/10.1007/978-3-642-36833-2_15.
Mazot, A., Schwandner, F.M., Christenson, B., de Ronde, C.E.J., Inguaggiato, S., Scott, B., Graham, D., Britten, K., Keeman, J., and Tan, K., 2014, CO_2 discharge from the bottom of volcanic lake Rotomahana, New Zealand: Geochemistry Geophysics Geosystems, v. 15, p. 577–588, https://doi.org/10.1002/2013GC004945.
McKenzie, J.A., 1985, Carbon isotopes and productivity in the lacustrine and marine environment, *in* Stumm, W., ed., Chemical Processes in Lakes: New York, Wiley, p. 99–118.
NIDIS (National Integrated Drought Information System), 2020, Current U.S. drought monitor conditions for Oregon: https://www.drought.gov/drought/states/oregon (accessed September 2020).
Oren, A., Gurevich, P., Anati, D.A., Barkan, E., and Luz, B., 1995, A bloom of *Dunaliella parva* in the Dead Sea in 1992: Biological and biogeochemical aspects: Hydrobiologia, v. 297, p. 173–185, https://doi.org/10.1007/BF00019283.
Pérez, N.M., et al., 2011, Global CO_2 emissions from volcanic lakes: Geology, v. 39, p. 235–238, https://doi.org/10.1130/G31586.1.
Pierrot, D.E.L., and Wallace, D.W.R., 2006, MS Excel program developed for CO_2 system calculations: Oak Ridge, Tennessee, U.S. Department of Energy, Oak Ridge National Laboratory, Carbon Dioxide Information Analysis Center, ORNL/CDIAC-105a, https://cdiac.ess-dive.lbl.gov/ftp/co2sys/CO2SYS_calc_XLS_v2.1/ (accessed September 2018).
Price, R.E., LaRowe, D.E., Italiano, F., Savov, I., Pichler, T., and Amend, J.P., 2015, Subsurface hydrothermal processes and the bioenergetics of chemolithoautotrophy at the shallow-sea vents off Panarea Island (Italy): Chemical Geology, v. 407–408, p. 21–45, https://doi.org/10.1016/j.chemgeo.2015.04.011.
Rouwet, D., Tassi, F., Mora-Amador, R., Sandria, L., and Chiarini, V., 2014, Past, present and future of volcanic lake monitoring: Journal of Volcanology and Geothermal Research, v. 272, p. 78–97, https://doi.org/10.1016/j.jvolgeores.2013.12.009.
Liu, T., Zhou, W., and Cheng, P., and Burr, G.S., 2018, A survey of the ^{14}C content of dissolved inorganic carbon in Chinese lakes: Radiocarbon, v. 60, p. 705–716, https://doi.org/10.1017/RDC.2017.113.
Tranvik, L.J., et al., 2009, Lakes and reservoirs as regulators of carbon cycling and climate: Limnology and Oceanography, v. 54, p. 2298–2314, https://doi.org/10.4319/lo.2009.54.6_part_2.2298.
USGS (U.S. Geological Survey), 2020, Low lake water, dry conditions in Newberry caldera the cause of increased sulfur smells? [news report, 7 August 2020]: https://www.usgs.gov/center-news/low-lake-water-dry-conditions-newberry-caldera-cause-increased-sulfur-smells.
Varekamp, J.C., 2015, The chemical composition and evolution of volcanic lakes, *in* Rouwet, D., et al., eds. Volcanic Lakes: Berlin, Heidelberg, Springer Media Publishers, p. 93–123, https://doi.org/10.1007/978-3-642-36833-2_4.

Printed in USA